Intrinsically switchable electroactive fluorophores based on λ5-biphosphinines

Thitiporn Sangchai, Nicolas Ledos, Antoine Vacher, Marie Cordier, Boris Le Guennic, Muirel Hissler, Denis Jacquemin, Pierre-Antoine Bouit

Chemistry–A European Journal
Research Article
doi.org/10.1002/chem.202301165
Chemistry Europe
European Chemical Societies Publishing
www.chemeurj.org

Intrinsically Switchable Electroactive Fluorophores Based on λ^5-Biphosphinines**

Thitiporn Sangchai,[a] Nicolas Ledos,[a] Antoine Vacher,[a] Marie Cordier,[a] Boris Le Guennic,[a] Muriel Hissler,[a] Denis Jacquemin,*[b, c] and Pierre-Antoine Bouit*[a]

Abstract: The synthesis and full characterization of a family of stable λ^5-biphosphinines connected in 4,4-position through a variety of π-conjugated bridges is reported. The impact of the π-bridge on the optical (absorption/emission) and redox properties was investigated using a joint experimental/theoretical approach. In contrast to the π-extended ones, the λ^5-biphosphinines directly connected through a C–C bond in 4,4-position display two easily accessible and reversible oxidations highlighting their multi-stage redox character. The in situ formed radical cations are studied by spectro-electrochemistry and electron paramagnetic resonance. Finally, electrochemical modulation of fluorescence (electrofluorochromism) was performed and revealed the potential of these intrinsically switchable electroactive fluorophores for further applications as switchable materials.

Introduction

Organic redox systems are molecules that are both investigated for fundamental purposes (electron transfer processes and reactivity) and used in applied materials science (conducting materials, photovoltaic devices, batteries or spintronic).[1] A common strategy to design such compounds is to link two heteroatoms through a π-bridge displaying an even number of sp^2 carbon atoms.[2] Such derivatives are called "Weitz type" redox systems and typically display three stable redox states. Among them, tetrathiafulvalene and methyl-viologens (MV) are the most widely used electron donors and electron acceptors, respectively.[3] Although the applicability of this strategy to phosphorus as the single heteroatom was postulated back in 1978,[2] organophosphorus multi-stage Weitz-type redox derivatives were described by our group in 2020 only (Figure 1).[4] In that work, we reported a family of dicationic P-containing Polycyclic Aromatic Hydrocarbons (PAHs), such as **A** (Figure 1) which displays three stable redox states including a radical cation. In contrast to MV, which are poorly luminescent, their intense luminescence was used in electrofluorochromic devices emitting in both the visible and near infrared domains.[5] This illustrated that the Weitz-strategy adapted to P-derivatives is an original way to obtain intrinsically switchable electroactive fluorophores[6] and overcome some limitations of widely used compounds such as MV. In order to prepare similar fluorophores which properties could be addressed upon oxidation (rather than reduction, as for **A**), a stable bis-ylide linked by an even number of sp^2 carbons has to be prepared according to general formula displayed in Figure 1. In the field of conjugated ylide, the λ^5-phosphinines (also called λ^5-phosphabenzene) recently appeared as a powerful building block for optoelectronic, following the pioneering observations by Müller et al.[7] Indeed, their intense luminescence was used in various optoelectronic devices such as organic light-emitting diodes and organic lasers.[8,9] In particular, the 2,6-dicarbonitrile diphenyl-1-λ^5-phosphinine scaffold (DCNP, blue heterocycle in **B**, Figure 1), firstly developed by Hayashi et al.,[9a] emerged as particularly interesting due to its straightforward synthesis, high stability, and easily tunable optical properties. However, their redox properties remain underexplored.

We thus decided to prepare λ^5-biphosphinines based on DCNP linked through their 4,4-position (see target **B**, Figure 1) to develop fluorescent multi-stage electron donors. In this article, we report the straightforward synthesis of a family (**2**–**6**, Schemes 1 and 2) where two ylidic P atoms are connected through various π-backbones featuring an even number of sp^2 carbons. The impact of the bridge on both the optical (absorption/emission) and redox properties, and in particular the presence of three redox states, is investigated using a joint experimental/theoretical approach. Finally, electrofluorochromic study was used to prove that these λ^5-biphosphinines behave as intrinsically switchable electroactive fluorophores and can be

[a] T. Sangchai, Dr. N. Ledos, Dr. A. Vacher, M. Cordier, Dr. B. Le Guennic, Prof. M. Hissler, Dr. P.-A. Bouit
Univ Rennes, CNRS, ISCR – UMR 6226
35000 Rennes (France)
E-mail: pierre-antoine.bouit@univ-rennes.fr

[b] Prof. D. Jacquemin
Nantes Université, CNRS, CEISAM UMR 6230
44000 Nantes (France)
E-mail: Denis.Jacquemin@univ-nantes.fr

[c] Prof. D. Jacquemin
Institut Universitaire de France (IUF)
75005 Paris (France)

[**] A previous version of this manuscript has been deposited on a preprint server (https://doi.org/10.26434/chemrxiv-2023-5ks97).

Supporting information for this article is available on the WWW under https://doi.org/10.1002/chem.202301165

Research Article
doi.org/10.1002/chem.202301165
Chemistry Europe
European Chemical Societies Publishing

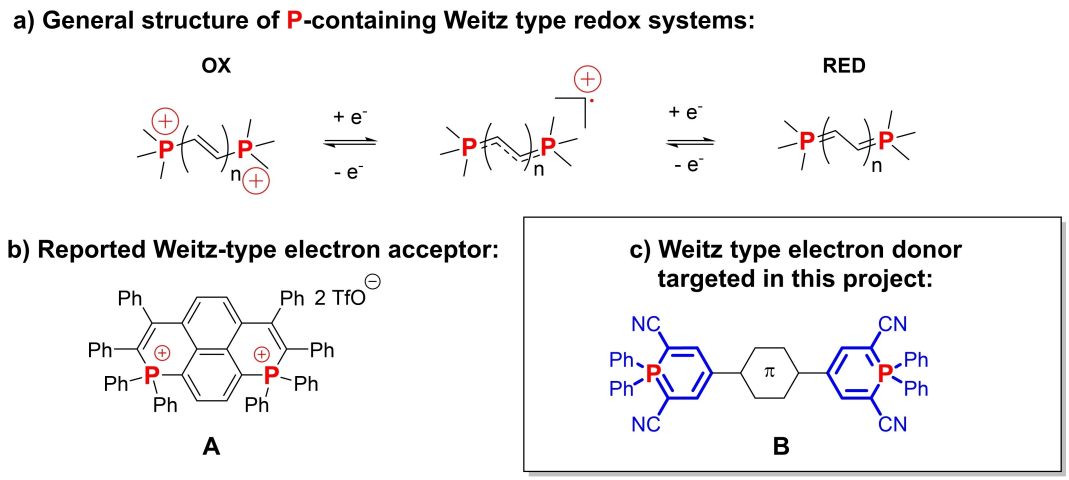

Figure 1. General structure of P-containing Weitz type redox systems (a), reported structure of electron acceptor using this strategy (b) and electron donor targeted in this article (c).

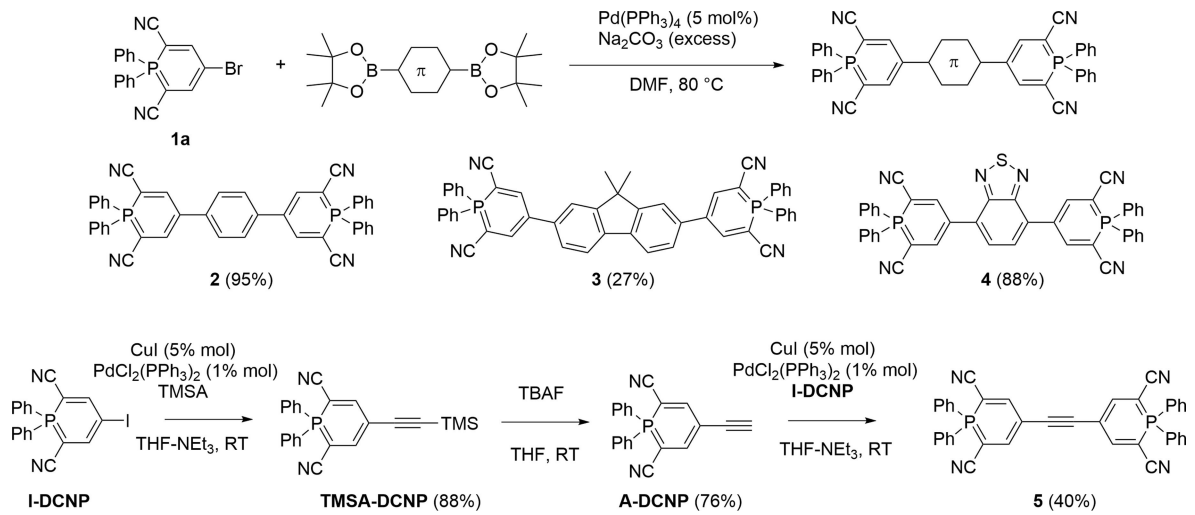

Scheme 1. Synthesis of π-extended λ^5-biphosphinines **2**–**5**.

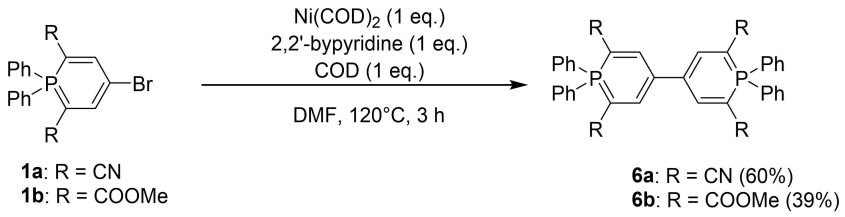

Scheme 2. Synthesis of directly connected λ^5-biphosphinines **6a**–**b**.

used for their redox properties, in addition to their recognized potential for luminescence.

Results and Discussion

To prepare our family of λ^5-biphosphinines,[10] we relied on the molecular engineering of DCNP, which is a highly stable ylidic fluorophore with great synthetic versatility. Our first approach is based on cross-coupling reactions starting from Br-DCNP **1a**[9a] (Scheme 1). To prepare the λ^5-biphosphinines linked through

various π-bridges, Br-DCNP **1a** was subjected to Pd-catalyzed cross-coupling with the corresponding dioxaborolane to afford λ^5-biphosphinines **2**–**4** in moderate to excellent yields (Scheme 1). Compound **5**, bridged by an alkyne, was prepared in moderate yields according to an iterative sequence of Sonogashira coupling and deprotection (Scheme 1).

For the preparation of λ^5-biphosphinines directly connected through a C–C bond in 4,4 position, that is **6a**–**b**,[11,12] we first relied on an oxidative coupling strategy (with either $FeCl_3$, $MoCl_3$ or DDQ/$MeSO_3H$) applied directly on DCNP.[13] However, after various unsuccessful tries, we turned to Ni-mediated Yamamoto coupling starting from bromo-DCNP **1a**. After optimization of the conditions, this approach led to the preparation of the targeted λ^5-biphosphinines **6a** and **6b** in satisfying yields (Scheme 2).

All compounds **2**–**6a**–**b** are fully air and moisture stable and soluble in most organic solvents. They were fully characterized by multinuclear NMR, high resolution mass spectrometry, and X-ray diffraction (see below).

The structures of **2**–**4** and **6a**–**b** were additionally confirmed by single-crystal X-ray diffraction (Figure 2, Figures S2–6, Table S2). In all compounds, the bond lengths within the λ^5-phosphinines are within expectations and attest the conjugated ylidic nature of the P–C bond ($1.75 < d_{P\text{-}C} < 1.77$ Å) while the intracyclic C–C bonds are nearly equalized (1.38 Å $< d_{C\text{-}C} <$ 1.40 Å).[7] The P-rings are globally planar as the maximal deviation from the mean plane is only 0.07 Å. As expected, a tilt angle is always observed between the two lateral λ^5-phosphinines (26.6° for **6a** and 32.5° for **6b**) or between the λ^5-phosphinines and its neighbouring aromatic ring (see Figure 2). The bond in *para* position between the two λ^5-phosphinine rings in **6a**–**b** is a pure C–C single bond ($d \sim 1.49$ Å, Table S2), confirming that each λ^5-phosphinine moiety keeps its (low) aromatic nature. No intermolecular interactions are observed in the packing due to the bulkiness of the two P–Ph exocyclic fragments. These data confirm that the DCNP fragments in all the λ^5-biphosphinines retain its characteristic structural features.

The optical properties of **2**–**6a**–**b** were investigated in diluted DCM solutions ($c = 5.10^{-6}$ mol.L^{-1}, Figure 3, Figure S7–12 and Table 1). All λ^5-biphosphinines **2**–**6a**–**b** display absorption spectra with an intense band at ca. 490 nm (Figure 3 and Table 1) characteristic of DCNP derivatives, that is only slightly redshifted compared to pristine DCNP ($\lambda = 458$ nm).[9a] Replacing the cyano in **6a** by esters in **6b** leads to a small redshift of 10 nm. In all these systems, this absorption band is assigned to π-π* excitations mainly centered on the λ^5-phosphinine rings. However, in **4**, the central benzothiadiazole unit plays the role of an acceptor (see theory below). The impact of the bridge is more striking on the luminescence (Figure 3 and Table 1), with a strong redshift compared to pristine DCNP ($\lambda_{em} = 491$ nm) observed for all compounds. When aromatic spacers are introduced, a gradual redshift is observed in the **2**/**3**, and **4** series leading to a large Stokes shift of 6300 cm^{-1} in **4**.

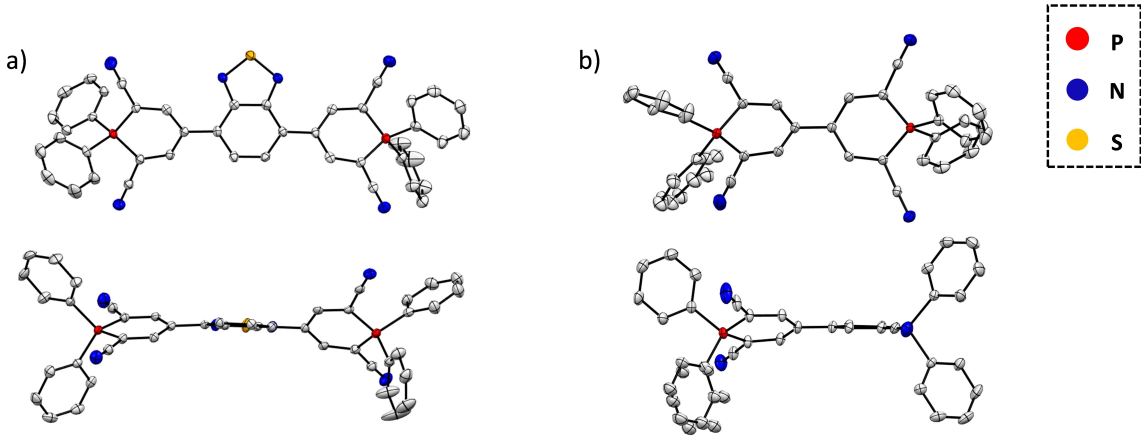

Figure 2. X-ray structure of **4** (a) and **6a** (b). Hydrogen atoms are omitted for clarity and thermal ellipsoids are set at 50% probability.

Table 1. Spectroscopic and electrochemical data.

Cpd	λ_{abs} [nm][a]	ε_{max} [M^{-1} cm^{-1}][a]	ε_{max} [M^{-1} cm^{-1}][a]	Φ_F [a,b]	$\lambda_{0\text{-}0}$ [nm][a]	σ [cm^{-1}][a]	$E^{ox\,1}$ [V vs DmFc][b]	$E^{ox\,2}$ [V vs DmFc][c]	E^{red} [V vs DmFc][c]
2	486	19000	562	0.43	522	2782	+1.03[d]	–	−1.60
3	488	17000	560	0.46	523	2634	+1.02[d]	–	−1.67
4	480	33000	688	0.05	560	6298	+1.01[d]	–	−1.36[d]
5	489	24000	588	0.23	542	3443	+0.87	+1.23[d]	−1.52
6a	494	15000	633	0.02	551	4445	+0.85 [d]	+1.05[d]	−1.53
6b	504	24000	655	0.04	574	4574	+0.46[d]	+0.71[d]	–

[a] In DCM (5.10^{-6} M). [b] Measured in calibrated integration sphere [c] ($c = 10^{-3}$ M) recorded in DCM with Bu_4NPF_6(0.2 M) at a scan rate of 200 mVs^{-1}. Potentials vs DmFc$^+$/DmFc. [d] quasi reversible processes.

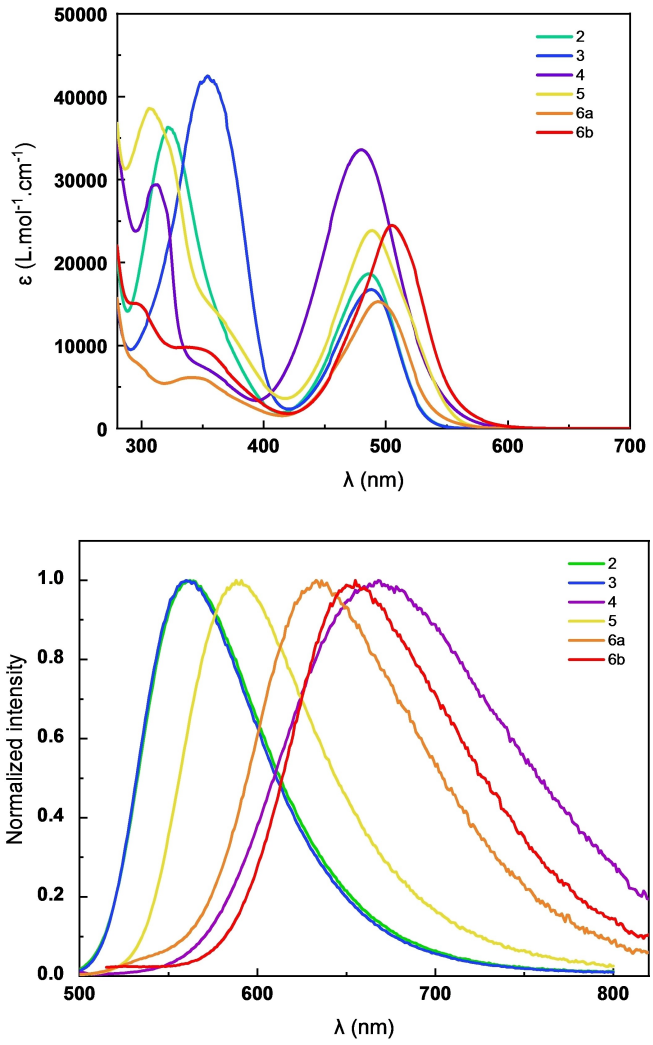

Figure 3. UV-Vis absorption (top) and normalized emission spectra (bottom) of **2**–**6a**–**b** in DCM ($c = 5.10^{-6}$ M).

Interestingly, the directly connected λ^5-biphosphinines **6a** and **6b** display emission bands that are redshifted as compared to λ^5-biphosphinines with phenylene/fluorenylene (**2**/**3**) or with an alkyne (**5**). Finally, replacing the cyano groups by esters in **6b** again leads to a small bathochromic shift of ca. 20 nm. This trend in luminescence wavelength comes with a general decrease in quantum yields where only **2**–**3** are efficient emitters ($\varphi \sim 0{,}45$). This is in global agreement with the energy gap law though **4** still delivers a relatively bright emission ($\varphi \sim 0{,}05$) for a dye emitting at nearly 700 nm in contrast to both **6a** and **6b** (Table 1).

We have used Time-Dependent Density Functional theory (TD-DFT) to probe the nature of the excited states of these compounds (see the Supporting Information for details). First, the ground-state geometries of all dyes investigated herein belong to the highest point group that can be reasonably envisaged (up to C_{2h} for **2** and **5** and D_2 for both **6a** and **6b**). For absorption, the presence of two identical weakly-coupled chromophores and this symmetry typically yield two low-lying excited states with almost identical transition energies but different transition probabilities (see Table S3). If one considers the most intense absorption transition, the relative shifts for the new compounds as compared to DCNP reasonably fit experiment, with, for example, TD-DFT values of +21 nm for **2** and +50 nm **6b**, respectively, that agree with the measured values of +28 nm and +46 nm. Importantly, both theory and experiment find that all new systems **2**–**6a**–**b** absorb at rather similar wavelengths. In Figure 4, we provide electron density difference (EDD) plots for selected transitions (see Figure S33 for all cases). In most cases, these EDD indicate that the excited-state has an almost additive character, with two DCNP-like excitations.[9d] This is clear for both **3** and **6b** shown in Figure 4. Compound **4** constitutes a clear exception as the lowest excitation involves a charge-transfer (CT) from the two lateral λ^5-phosphinine moieties towards the central benzothiadiazole core. This CT state is however appearing at a very close energy to the DNCP-localized transition (Table S3) and it is likely that the observed absorption band encompasses three close-lying excited states (Table S3). For the emission, the relaxation of the excited-state geometries sometimes leads to symmetry breaking, making the analysis more complex, see Table S4 in the Supporting Information. TD-DFT predicts that **4** leads to the most redshifted fluorescence (656 nm with a very large *f* indicating a large radiative rate), consistent with the data of Table 1 that shows a non-trifling emission at 688 nm. In contrast for both **6a** and **6b**, the minimization of the excited-state structure yields similar fluorescence wavelengths (534 and 554 nm, respectively) but associated with negligible transition probabilities, explaining the very low quantum yields that have been observed. For both **2** and **3**, the relaxation effects are much less marked leading to similar fluorescence wavelengths for the two systems and also smaller Stokes shift, again consistent with experimental trends.

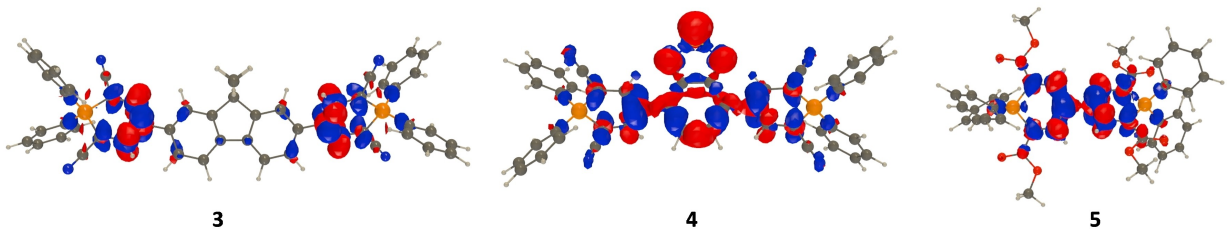

Figure 4. Electron density difference computed for the lowest transition of **3** (left), **4** (middle) and **6b** (right). The blue and red regions respectively indicate decrease and increase of density upon photon absorption (contour threshold: 0.001 au). See the Supporting Information for the other transitions.

In short, the fact that the absorption bands in Figure 3 are all similar whereas much stronger variations across the series are found for the emission bands in Figure 4 is related to the presence of two nearly equivalent λ^5-phosphinine moieties and the emergence of symmetry breaking in several cases. As a final note for **3**, the intense band experimentally observed at ca. 350 nm (Figure 3) corresponds to a π-π^* transition delocalized over the full molecule (see the Supporting Information).

The electrochemical behaviour of **2**–**6ab** was investigated by cyclic voltammetry in DCM solution (Figure 5, Figure S13-19). λ^5-Biphosphinines featuring aromatic spacers **2**–**4** display only a single two electron reversible oxidation at ca. +1 V vs $DmFc^+$/DmFc (decamethylferrocenium/decamethylferrocene) (see Figure 5 and Table 1). Such values fit with the oxidation reported for *para*-substituted DCNP derivatives.[14] As observed in extended MV derivatives, the presence of aromatic π-linkers leads to a single redox process in the corresponding λ^5-biphosphinines, indicating the absence of significant electronic communication between the two end-groups.[15] Note that the presence of the electro-withdrawing benzothiadiazole in **4** leads to the presence of a quasi-reversible reduction, making **4** an amphoteric redox system (Figure S16). The presence of the alkyne linker in **5** surprisingly leads to a fully irreversible oxidation process (Figure S17).[16] Finally, the directly connected λ^5-biphosphinines **6a** and **6b** a display distinct behaviour compared to **2**–**5**. Contrary to the previously studied derivatives, they both display two distinctively separated reversible oxidation waves at lower potential (e.g., Eox_1(**6b**) = +0.46 V vs $DmFc^+$/DmFc and Eox_2(**6b**) = +0.71 V vs $DmFc^+$/DmFc, Figure 5 and Table 1), characteristic of Weitz-type redox systems. This finding suggests the successive formation of a radical cation and a dicationic specie. Replacing the cyano groups of **6a** by esters in **6b** leads to a decrease in oxidation potential of 400 mV, consistent with the redshift observed in UV-Vis absorption. Compared to simple para-substituted λ^5-phosphinine such as **Ph-DCNP**[9a] (Figure S13), the molecular design of **6a**–**b** leads to a decrease in oxidation of almost 1 V. Such oxidation potentials range is similar to the tetrathiafulvalenes, probably the most widely used multi-stage redox system addressable in oxidation.[3b,c] This univocally validates our design strategy of preparing λ^5-biphosphinines as electron rich multi-stage redox systems.

To gain deeper insights into the properties of these novel multi-stage electron donors, spectroelectrochemical and electron paramagnetic resonance (EPR) measurements were performed for both **6a** and **6b** (Figure S20–25). Illustratively, each redox state of **6b** displays characteristic UV-Vis absorption signature. The absorption of radical cation $\mathbf{6b}^{+\bullet}$ is characterized by the appearance of redshifted transitions (λ = 750 nm, Figure 6), which are characteristic of a π-delocalized radical. Upon further oxidation toward the dicationic form, this low energy absorption disappears and a new transition rises at 398–414 nm (Figure 6). Vertical TD-DFT calculations for the $\mathbf{6b}^{+\bullet}$ and $\mathbf{6b}^{2+}$ species respectively yield the lowest absorption band at 707 nm (f = 0.803) and 399 nm (f = 1.908) which is obviously consistent with the measurements. The EDD plots for these transitions are available in the Supporting Information (Figure S33). The initial spectrum of **6b** was recovered upon restoring the starting potential (Figure S25), demonstrating the reversibility of the process. A similar behavior is observed for **6a** (Figures S21–22). EPR spectrum (g = 2.001) was recorded in DCM at 77 K after chemical oxidation of **6b** with nitrosonium hexafluorophosphate (Figure 6) confirming the formation of an organic radical. The structure of the spectrum is reproduced considering the coupling of the unpaired electron with the two equivalent phosphorus atoms (the four equivalent protons only lead to unresolved broad signals) (Figure S32). This evidences that the radical is delocalized on the entire π-system. Indeed, the computed spin density displayed in Figure 6, shows a symmetric distribution delocalized over the two λ^5-phosphinine groups. Again, similar behavior is observed for **6a** (Figure S29–30).

As evidenced during the optical/redox study, **6a** and **6b** are intrinsically fluorescent, contrary to TTF derivatives,[3b,c] and they can be reversibly oxidized giving rise to stable radicals. To take advantage of this specific property, we investigated the redox modulation of the luminescence of **6b** in DCM solution in a homemade electrofluorochromic set up (see the Supporting

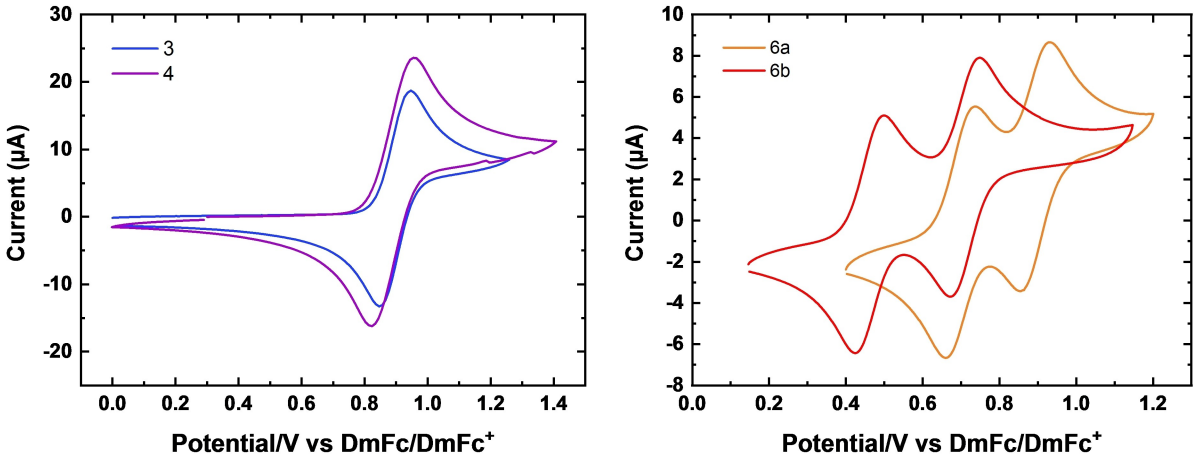

Figure 5. Cyclic voltammograms of **3** and **4** (left), **6a** and **6b** (right) ($c = 10^{-3}$ M) in DCM (Bu_4NPF_6 (0.2 M), 200–mVs^{-1}, potentials vs $DmFc^+$/DmFc).

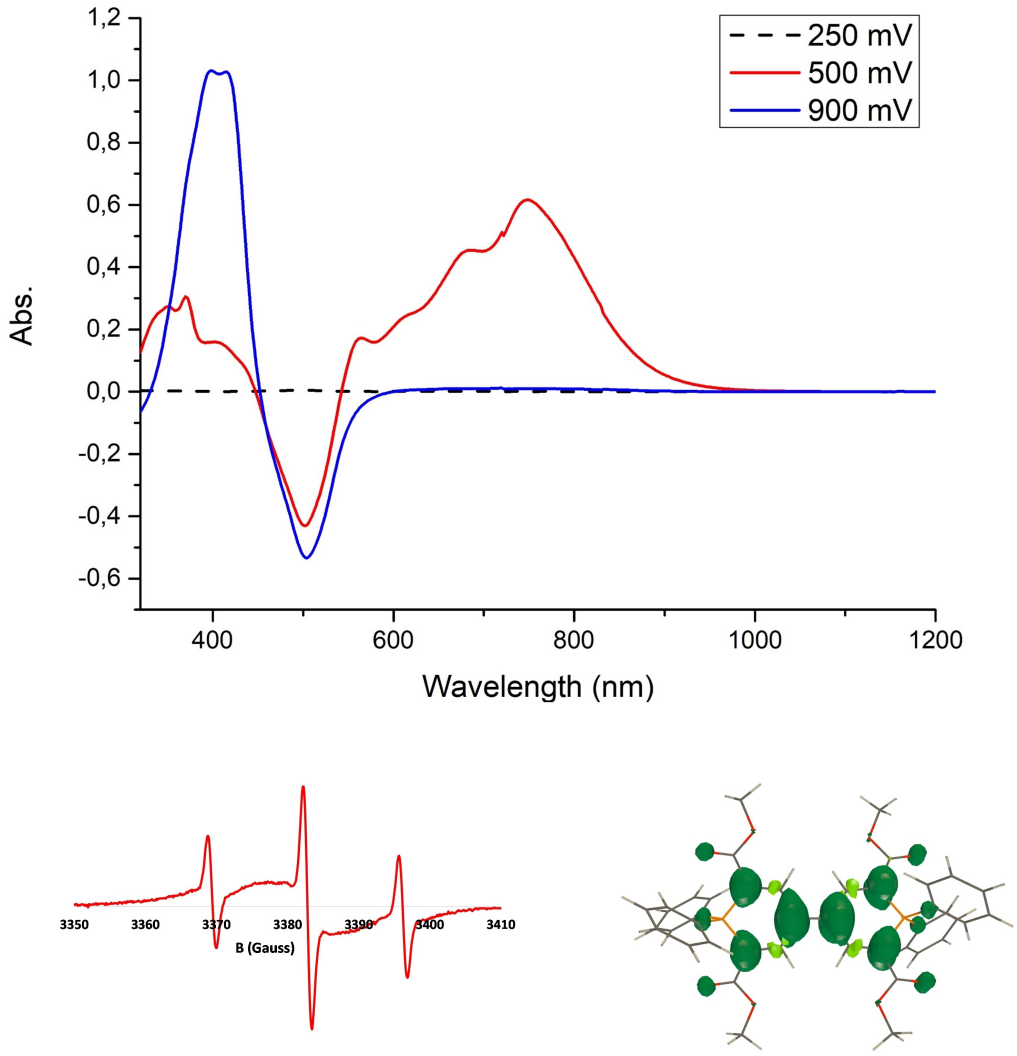

Figure 6. Differential absorption measured during the electrochemical oxidation of **6b** ($c = 5.10^{-4}$ M) in a solution of Bu_4NPF_6 (0.2 m) in DCM (up) EPR of the chemically generated **6b**$^{+\bullet}$ in DCM at 77 K (bottom left). (c) Spin density in **6b**$^{+\bullet}$ (bottom left, threshold 0.002 au).

Information). As illustrated in Figure 7, the application of +400 mV vs Pt allowed to switch off the red luminescence of **6b**. The luminescence was then restored upon reversal of the potential (−500 mV vs Pt). To illustrate the reversibility of the process, the luminescence of **6b** was successfully turned off and on (see Figure 7 and Figure S27) upon applying a sequence of oxidation (+500 mV vs Pt) and reduction (−500 mV vs Pt). These preliminary results indicate that λ^5-biphosphinines can be viewed not only as an emerging class of fluorophores usable in OLEDs/lasers but can also likely find applications related to their appealing redox properties, as illustrated by these electro-fluorochromic properties. In addition, it extends the scope of Weitz-type organophosphorus derivatives by showing that they can operate under oxidative quenching.

Conclusions

In short, we report the synthesis and full characterization of a family of λ^5-biphosphinines **2**–**6** based on the DCNP scaffold directly connected through a C–C bond or through various π-linkers in the 4,4 position. For the design, we relied on the Weitz type strategy where two ylidic P atoms are connected through a π-skeleton displaying an even number of sp^2 carbons. Based on a combined experimental and theoretical study, we show that while the absorption is moderately impacted by the nature of the linker, both the emission and the redox properties are strongly dependent on its nature. In particular, the two directly connected λ^5-biphosphinines **6a**–**b** display two easily accessible and reversible oxidations, making them appealing multi-stage redox systems. Finally, the fluorescence of **6b** was electrochemically modulated unambiguously showing that these λ^5-biphosphinines behave as intrinsically switchable electroactive fluorophores. While DCNP derivatives are becoming an attractive class of photonic dyes, these first electro-

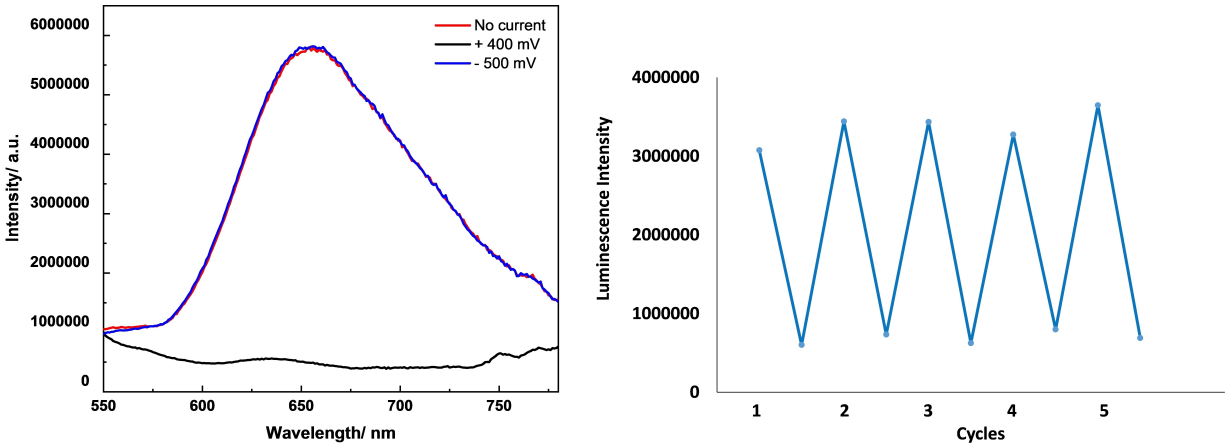

Figure 7. Modulation of fluorescence intensity upon oxidation of compounds **6 b** (left); $I_{654\,nm}$ switching (right).

fluorochromism results illustrate the potential of this family for applications as luminescent switches or in typical functions of multi-stage redox systems (photocatalysis,[17] spintronics,[18] energy storage[19]).

Experimental Section

Experimental procedures, NMR data, optical and redox characterizations and theoretical data are available in Supporting Information.

Deposition Numbers 2207046 (**2**), 2207045 (**3**), 2207044 (**4**), 2207047 (**6 a**), and 2207048 (**6 b**) contain the supplementary crystallographic data for this paper. These data are provided free of charge by the joint Cambridge Crystallographic Data Centre and Fachinformationszentrum Karlsruhe Access Structures service.

Additional references cited within the Supporting Information.[20–27]

Acknowledgements

This work is supported by the Ministère de la Recherche et de l'Enseignement Supérieur, the CNRS, the Région Bretagne (ARED grant to NL), the French National Research Agency (ANR Fluohyb ANR-17-CE09-0020), the GDR Phosphore. G. Taupier (Scanmat-UMS 2001) is thanked for PLQY measurements. T. Guizouarn (ISCR) is thanked for assistance with the EPR measurements. DJ is indebted to the CCIPL/Glicid computational center for the very generous allocation of computational time.

Conflict of Interests

The authors declare no conflict of interest.

Data Availability Statement

The data that support the findings of this study are available from the corresponding author upon reasonable request.

Keywords: Electrofluorochromism · luminescence · organophosphorus · radical · redox systems

[1] T. Nishinaga, *Organic Redox Systems: Synthesis, Properties, Applications*, Wiley-VCH, Weinheim, Germany **2015**.
[2] a) S. Hünig, S. H. Berneth, *Two step reversible redox systems of the Weitz type In: Organic Chemistry. Topics in Current Chemistry*, Vol 92. Springer, Berlin, Heidelberg **1980**; b) K. Deuchert, S. Hünig, *Angew. Chem. Int. Ed.* **1978**, *17*, 875–886.
[3] a) L. Striepe, T. Baumgartner, *T. Chem. Eur. J.* **2017**, *23*, 16924–16940; b) J. L. Segura, N. Martin, *Angew. Chem. Int. Ed.* **2001**, *40*, 1372–1409; c) D. Canevet, M. Sallé, G. Zhang, D. Zhang, D. Zhu, *Chem. Commun.* **2009**, 2245–2269.
[4] T. Delouche, A. Vacher, E. Caytan, T. Roisnel, B. Le Guennic, D. Jacquemin, M. Hissler, P.-A. Bouit, *Chem. Eur. J.* **2020**, *26*, 8226–8229.
[5] T. Delouche, A. Vacher, T. Roisnel, M. Cordier, J.-F. Audibert, B. Le Guennic, F. Miomandre, D. Jacquemin, M. Hissler, P.-A. Bouit, *Mater Adv* **2020**, *1*, 3369–3377.
[6] a) P. Audebert, F. Miomandre, *Chem. Sci.* **2013**, *4*, 575–584; b) H. Al-Kutubi, H. R. Zafarani, L. Rassaei, K. Mathwig, *Eur. Polym. J.* **2016**, *83*, 478–498; c) A. Beneduci, S. Cospito, M. La Deda, G. Chidichimo, *Adv. Funct. Mater.* **2015**, *25*, 1240–1247; d) F. Miomandre, *Curr. Opin. Electrochem.* **2020**, *24*, 56–62.
[7] C. Müller, D. Wasserberg, J. J. M. Weemers, E. A. Pidko, S. Hoffmann, M. Lutz, A. L. Spek, S. C. J. Meskers, R. A. J. Janssen, R. A. van Santen, D. Vogt, *D. Chem. Eur. J.* **2007**, *13*, 4548.
[8] a) G. Pfeifer, F. Chahdoura, M. Papke, M. Weber, R. Szücs, B. Geffroy, D. Tondelier, L. Nyulászi, M. Hissler, C. Müller, *Chem. Eur. J.* **2020**, *26*, 10534; b) T. Delouche, E. Caytan, M. Cordier, T. Roisnel, G. Taupier, Y. Molard, N. Vanthuyne, B. Le Guennic, M. Hissler, D. Jacquemin, P.-A. Bouit, *Angew. Chem. Int. Ed.* **2022**, *61*, e202205548.
[9] a) N. Hashimoto, R. Umano, Y. Ochi, K. Shimahara, J. Nakamura, S. Mori, H. Ohta, Y. Watanabe, M. Hayashi, *J. Am. Chem. Soc.* **2018**, *140*, 2046–2049; b) B. S. B. Karunathilaka, U. Balijapalli, C. A. M. Senevirathne, Y. Esaki, K. Goushi, T. Matsushima, A. S. D. Sandanayaka, C. Adachi, *Adv. Funct. Mater.* **2020**, *30*, 2001078; c) X. Tang, U. Balijapalli, D. Okada, B. S. B. Karunathilaka, C. A. M. Senevirathne, Y. Lee, Z. Feng, A. S. D. Sandanayaka, T. Matsushima, C. Adachi, *Adv. Funct. Mater.* **2021**, *31*, 2104529; d) N. Ledos, T. Sangchai, I. Knysh, M. H. E. Bousquet, P. Manzhi, M. Cordier, D. Tondelier, B. Geffroy, D. Jacquemin, P.-A Bouit, Muriel Hissler, *Org. Lett.* **2022**, *24*, 6869–6873; e) B. S. B. Karunathilaka, U. Balijapalli, C. A. M. Senevirathne, S. Yoshida, Y. Esaki, K. Goushi, T.

Matsushima, A. S. D. Sandanayaka, C. Adachi *Nat. Commun.* **2020**, *11*, 4926.
[10] Non-conjugated para-substituted λ^5-phosphinines have been previously reported: W. Schafer, K. Dimroth, *Tetrahedron Lett.* **1972**, *9*, 843–846, as well as conjugated para-substituted λ^3-phosphinines: G. Märkl, D. E. Fischer, H. Olbrich, *Tetrahedron Lett.* **1970**, *9*, 645–648.
[11] M. Hayashi, H. Ohta, K. Yoneda, WO2021152868 A1 2021–08-05.
[12] The structure of 6b with the ester groups is inspired by the design of MV stable radicals: M. Berville, J. Richard, M. Stolar, S. Chaoua, N. Le Breton, C. Gourlaouen, C. Boudon, L. Ruhlmann, T. Baumgartner, J. A. Wytko, J. Weiss, *Org. Lett.* **2018**, *20*, 8004–8008.
[13] M. Grzybowski, B. Sadowski, H. Butenshön, D. T. Gryko, *Angew. Chem. Int. Ed.* **2020**, *59*, 2998–3027.
[14] U. Balijapalli, X. Tang, D. Okada, Y. Lee, B. S. B. Karunathilaka, M. Auffray, G. Tumen-Ulzii, Y. Tsuchiya, A. S. D. Sandanayaka, T. Matsushima, H. Nakanotani, C. Adachi, *Adv. Opt. Mater.* **2021**, *9*, 2101122.
[15] G. Tang, Y. Liu, Y. Li, K. Peng, P. Zuo, Z. Yang, T. Xu, *JACS Au* **2022**, *2*, 1214–1222.
[16] Such phenomenon was also observed with Pt, C, and Au working electrodes.
[17] a) V. Quint, F. Morlet-Savary, J.-F. Lohier, J. Lalevée, A.-C. Gaumont, S. Lakhdar, *J. Am. Chem. Soc.* **2016**, *138*, 7436–7441; b) P. W. Antoni, M. M. Hansmann, *J. Am. Chem. Soc.* **2018**, *140*, 14823–14835; c) G. Li, L. Xu, W. Zhang, K. Zhou, Y. Ding, F. Liu, X. He, G. He, *Angew. Chem. Int. Ed.* **2018**, *57*, 4897–4901.
[18] a) Y. Huang, E. Egap, *Polym. J.* **2018**, *50*, 603–614; b) J. E. Barker, J. J. Dressler, A. Cárdenas Valdivia, R. Kishi, E. T. Strand, L. N. Zakharov, S. N. MacMillan, C. J. Gómez-García, M. Nakano, J. Casado, M. M. Haley, *J. Am. Chem. Soc.* **2020**, *142*, 1548–1555; c) T. Y. Gopalakrishna, W. Zeng, X. Lu, J. Wu, *Chem. Commun.* **2018**, *54*, 2186–2199.
[19] a) G. Li, B. Zhang, J. Wang, H. Zhao, W. Ma, L. Xu, W. Zhang, K. Zhou, Y. Du, G. He, *Angew. Chem. Int. Ed.* **2019**, *58*, 8468–8473; b) M. Stolar, C. Reus, T. Baumgartner, *Adv. Energy Mater.* **2016**, *6*, 1600944.
[20] J. Vicente, M. T. Chicote, I. Saura-LLamas, *Organometallics* **1989**, *8*, 767.
[21] M. J. Frisch, G. W. Trucks, H. B. Schlegel, G. E. Scuseria, M. A. Robb, J. R. Cheeseman, G. Scalmani, V. Barone, G. A. Petersson, H. Nakatsuji, X. Li, M. Caricato, A. V. Marenich, J. Bloino, B. G. Janesko, R. Gomperts, B. Mennucci, H. P. Hratchian, J. V. Ortiz, A. F. Izmaylov, J. L. Sonnenberg, D. Williams-Young, F. Ding, F. Lipparini, F. Egidi, J. Goings, B. Peng, A. Petrone, T. Henderson, D. Ranasinghe, V. G. Zakrzewski, J. Gao, N. Rega, G. Zheng, W. Liang, M. Hada, M. Ehara, K. Toyota, R. Fukuda, J. Hasegawa, M. Ishida, T. Nakajima, Y. Honda, O. Kitao, H. Nakai, T. Vreven, K. Throssell, J. A. Montgomery Jr., J. E. Peralta, F. Ogliaro, M. J. Bearpark, J. J. Heyd, E. N. Brothers, K. N. Kudin, V. N. Staroverov, T. A. Keith, R. Kobayashi, J. Normand, K. Raghavachari, A. P. Rendell, J. C. Burant, S. S. Iyengar, J. Tomasi, M. Cossi, J. M. Millam, M. Klene, C. Adamo, R. Cammi, J. W. Ochterski, R. L. Martin, K. Morokuma, O. Farkas, J. B. Foresman, D. J. Fox, Gaussian 16, revision A.03; Gaussian Inc.: Wallingford, CT **2016**
[22] J. D. Chai, M. Head-Gordon, *Phys. Chem. Chem. Phys.* **2008**, *44*, 6615–6620.
[23] J. Tomasi, B. Mennucci, R. Cammi, *Chem. Rev.* **2005**, *105*, 2999–3094.
[24] C. A. Guido, A. Chrayteh, G. Sclamani, B. Mennucci, D. Jacquemin *J. Chem. Theory Comput.* **2021**, *17*, 5155–5164.
[25] D. Jacquemin, A. Planchat, C. Adamo, B. Mennucci, *J. Chem. Theory Comput.* **2012**, *8*, 2359–2372.
[26] A. D. Laurent, D. Jacquemin, *Int. J. Quantum Chem.* **2013**, *113*, 2019–2039.
[27] A. D. Laurent, C. Adamo, D. Jacquemin, *Phys. Chem. Chem. Phys.* **2014**, *16*, 14334–14356.

Manuscript received: April 13, 2023
Accepted manuscript online: May 10, 2023
Version of record online: June 13, 2023